THE JOURNAL OF PHYSICAL CHEMISTRY A

 VOLUME 110, NUMBER 22, JUNE 8, 2006

ARTICLES

Dynamical Calculations of Charge-Transfer-to-Solvent Excited States of Small $I^-(CH_3CN)_n$ Clusters

Toshiyuki Takayanagi*

Department of Chemistry, Saitama University, 255 Shimo-Okubo, Sakura-ku, Saitama City, Saitama 338-8570, Japan

Received: March 6, 2006; In Final Form: April 6, 2006

Relaxation dynamics of photoexcited charge-transfer-to-solvent (CTTS) states for the $I^-(CH_3CN)_n$ ($n = 2$ and 3) clusters has been theoretically studied using electronic structure methods. First, we have calculated several lowest singlet and triplet potential energy surfaces using the multireference configuration interaction method. It was found that the character of the singlet CTTS excited-state potential surfaces is very similar to that of the triplet CTTS states. Due to a small singlet−triplet splitting, the lowest triplet potential energy surface was used as a good model to understand the dynamics of the photoexcited singlet CTTS states. We have carried out direct molecular dynamics simulations on the lowest triplet surface at the B3LYP level. When an I^- anion is exteriorly solvated by CH_3CN molecules, we found that the $(CH_3CN)_n^-$ anion cluster is effectively produced. In addition, when the I^- anion is placed in the interior in $I^-(CH_3CN)_n$ clusters, photoexcitation gives an acetonitrile monomer anion plus neutral monomers. However, if the initial geometric configuration is distorted from the minimum structure, we also found that the $(CH_3CN)_2^-$ anion cluster, where an excess electron is internally trapped, is formed via $I^-(CH_3CN)_2 + h\nu \rightarrow I + (CH_3CN)_2^-$ process.

I. Introduction

Solvation phenomena of excess electrons in condensed-phase polar molecules have been extensively studied from both experimental and theoretical points of view due to their basic importance in diverse fields of physics, chemistry, biology, and nanoscience.[1] It is well-known that photoexcitation of halide anions dissolved in polar solvent molecules is a particularly useful approach to study the dynamics of excess electrons in solvent molecules, because electronically excited states of this system are precursors of so-called charge-transfer-to-solvent (CTTS) states, where an excited electron is collectively stabilized by polar molecules and a solvated electron is finally produced after relaxation.[2−5] In addition, it should be emphasized that relaxation dynamics after CTTS excitation is a prototype of electron-transfer reactions in liquid phase.

To understand the solvation dynamics of excess electrons at a microscopic level, experimental studies using molecular clusters in the gas phase are known to be quite useful.[6] Recent advances in molecular beam techniques as well as laser spectroscopic techniques have revealed that useful information on the solvation dynamics can be obtained by systematically varying cluster size. Johnson and co-workers first succeeded in observing cluster analogues of the bulk CTTS states in clusters of an iodide anion with polar solvent molecules.[7−10] They have measured photoabsorption spectra of the I^-M_n (M is a polar solvent molecule) clusters and found that relaxation of the CTTS excited state leads to ejection of a neutral iodide atom and release of a negatively charged solvent cluster, $I^-M_n + h\nu \rightarrow [I^-M_n]^* \rightarrow I + M_n^-$. Neumark and co-workers have recently applied femtosecond spectroscopic techniques to the $I^-(H_2O)_n$ cluster system and reported the time evolution of excess electron

* E-mail address: tako@chem.saitama-u.ac.jp.

10.1021/jp061395x CCC: $33.50
Published on Web 05/13/2006

binding energies, which gives detailed information on the dynamics of the $(H_2O)_n^-$ anion cluster production.[11−17] In addition, Kim and co-workers[18−24] have recently carried out extensive electronic structure calculations for the $I^-(H_2O)_n$ clusters from the theoretical side.

We focus here on the relaxation dynamics of the CTTS excited states of the iodide−acetonitrile anion clusters. Although the $I^-(H_2O)_n$ clusters have been most extensively studied among various cluster systems from both experimental and theoretical points of view, it may be interesting to understand the differences in relaxation dynamics due to the change in solvent molecules. In addition, small iodide−acetonitrile clusters have also been studied experimentally in detail.[7,8] Photoelectron spectra of the $I^-(CH_3CN)_2^-$ cluster suggested the existence of two isomers: one with the solvent molecules surrounding the I^- anion (symmetric solvation) and another with both solvent molecules on the same side, asymmetrically solvating the I^- anion (asymmetric solvation). It has been concluded that excitation of the former cluster results in electron detachment, while excitation of the latter isomer results in production of both CH_3CN^- and $(CH_3CN)_2^-$ anions. Motivated by these experimental findings, we report theoretical studies on the relaxation dynamics of the CTTS excited states of the $I^-(CH_3CN)_2$ and $I^-(CH_3CN)_3$ clusters.

II. Computational Method

Potential energy curves of ground and excited electronic states for the $I^-(CH_3CN)_2$ cluster have been calculated with the multireference configuration interaction (MRCI) method. The molecular orbitals used in the MRCI calculations were obtained from the state-averaged complete-active-space self-consistent-field (SA-CASSCF) method, where the active space consists of one s orbital and three p orbitals of the iodide atom and the lowest unoccupied orbital, which accommodates the excited electron upon photoexcitation. Thus, six electrons were distributed among five active orbitals. For an I atom, a Stuttgart−Dresden−Bonn quasi-relativistic ECP46MWB effective core potential[25] with valence basis sets augmented by diffuse s and p as well as polarization d and f functions was used. The exponents for this basis set were taken from the paper of Glukhovtsev et al.[26] For C, N, and H atoms, the standard aug-cc-pVDZ basis sets[27] were employed, but additional diffuse functions were supplemented on the carbon atom in the methyl group of each acetonitrile molecule in clusters in order to effectively describe the diffuse nature of the loosely bound electrons. The exponents used for the s orbitals were 0.009 38, 0.001 876, and 0.000 375 2, while those used for the p orbitals were 0.008 082, 0.001 616 4, and 0.000 323 28.[28] These are scaled values of the outermost s and p orbitals of the aug-cc-pVDZ basis set of carbon with a progression factor of $^1/_5$. The spin−orbit interaction was completely ignored in this work. All MRCI calculations were performed using the MOLPRO program.[29]

As described below, we have carried out direct molecular dynamics trajectory calculations in order to understand the relaxation mechanism of the CTTS excited state of the $I^-(CH_3CN)_n$ anion cluster. The singlet CTTS excited states should have the same spin multiplicity as the ground state of the system. Thus, to perform such dynamics calculations, one has to employ, in principle, the electronic structure method that can properly describe both ground- and excited-state potential energy surfaces. The use of a multiconfigurational method such as CASSCF and CASPT2 would be desirable. In fact, Timerghazin and Peslherbe,[30] and Kołaski et al.[24] have recently reported the direct dynamics calculations of the photoexcited $I^-(H_2O)_3$ cluster using the CASSCF method, although they had to decrease the active space of the CASSCF calculations in order to reduce computational time. Unfortunately, the multiconfigurational calculations are computationally demanding and often cause SCF convergence problems. Instead, we have done direct dynamics calculations on the lowest triplet CTTS excited-state potential energy surface, since the features of the triplet surfaces are quite similar to those of the singlet CTTS excited states, as will be shown later. In this case, one can use the electronic structure method based on the single-reference approximation. This approach was also used in the theoretical work of Bradforth and Jungwirth.[31] They have calculated absorption spectra of iodide anions in bulk water on the basis of the MRCI calculations of Villa and Jordan.[32]

The direct trajectory calculations were carried out at the hybrid density functional UB3LYP level,[33] which was determined by compromise of computational costs and accuracy. We employed the BOMD (Born−Oppenheimer molecular dynamics) method implemented in the *Gaussian 03* package.[34] This method uses a fifth-order polynomial fitted to the energy, gradient, and Hessian at each time step, and then, the step size is taken to be much larger than the step size used in the normal method employing only the gradient information. The basis sets used in the BOMD calculations were chosen to be small to save computational time. For an iodide atom, the ECP46MWB effective core potential was employed, but diffuse and polarization functions were not added. For H, C, and N atoms, a standard 6-31+G(d) basis set has been employed, but two diffuse sp shells with exponents $\alpha_{sp} = 0.001\,46$ and 0.004 867 were added on carbon atoms in methyl groups. These exponents are scaled values of the outermost sp shell of the 6-31+G(d) basis set of carbon with a progression factor being $^1/_3$.[35,36]

III. Potential Energy Curves for the $I^-(CH_3CN)_2$ Cluster

Before presenting results of molecular dynamics calculations, it should be important to understand the features of the potential energy surfaces for the $I^-(CH_3CN)_n$ cluster in both the ground and excited electronic states. We have carried out ab initio MRCI calculations for the smallest $I^-(CH_3CN)_2$ cluster system. Previous theoretical calculations[37−39] have revealed that the $I^-(CH_3CN)_2$ cluster in the ground electronic state has two important minimum structures. The first isomer corresponds to a C_{3v}-like structure, in which the I^- anion is asymmetrically bound in the side position of the collinear head-to-tail acetonitrile dimer configuration (see also Figures 1 and 4). The other isomer has a D_{3d}-like structure, where the I^- anion is internally and symmetrically bound by two methyl groups of acetonitrile molecules. It is important to point out that the former configuration corresponds to the so-called surface state, while the latter structure to the internal state.

Figure 1a shows the MRCI potential energy curves as a function of the I−C distance (R) for the ground and excited states (three singlet and triplet CTTS excited states, respectively) of $I^-(CH_3CN)_2$ in the C_{3v}-like configuration as well as for the lowest three doublet states of the neutral $I(CH_3CN)_2$ cluster. Other internal coordinates were fixed to the values optimized by the MP2 level of the ground-state $I^-(CH_3CN)_2$ cluster with the same basis set. Actual calculations were done under the C_s point group. It is seen that the singlet excited-state potential curves are quite similar to the triplet potential curves, although the triplet states lie slightly lower in energy. It is interesting to note that the potential energy curves for the doublet neutral cluster are also very similar to those anion potential curves with

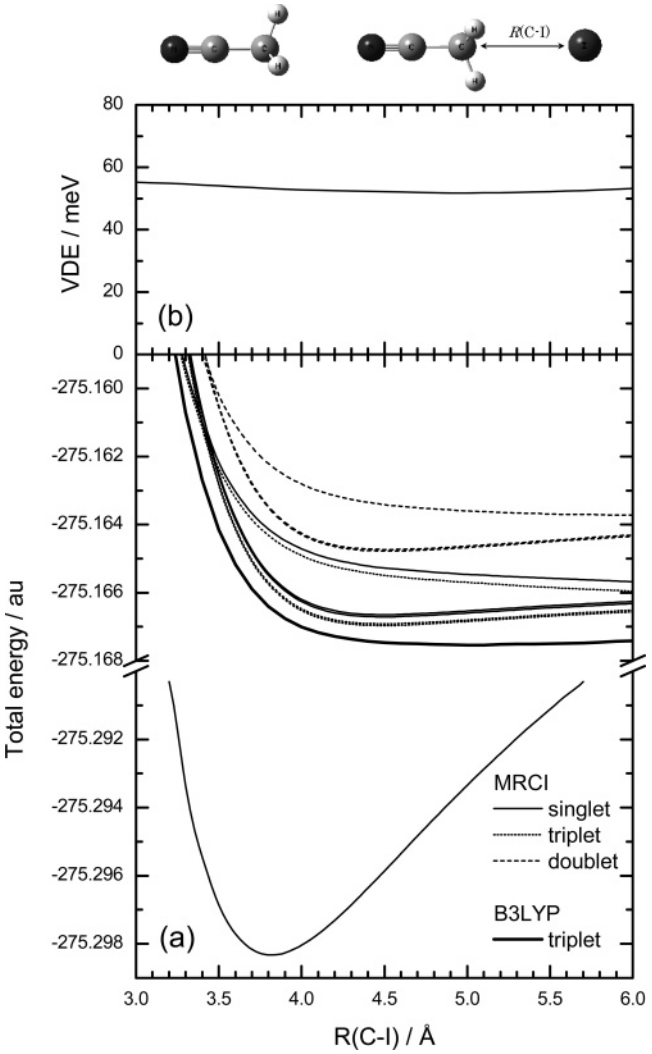

Figure 1. MRCI potential energy curves (a) as a function of the C−I distance for low-lying states of the $I^-(CH_3CN)_2$ and $I(CH_3CN)_2$ clusters with the C_{3v}-like surface configuration. Lowest four singlet curves (thin solid lines), lowest three triplet curves (dotted lines), and lowest three doublet curves (dashed lines) are plotted. B3LYP results for the lowest triplet state are shown as a bold line. The B3LYP energies are shifted to fit in this plot range. The vertical detachment energy (VDE) is also plotted in (b).

small energy shifts. For all spin multiplicity states, the lowest two curves show an attractive behavior, while the third state shows a repulsive character. However, it should be emphasized that interaction energy is quite small and that all the potential energy curves obtained are very flat in energy at least for $R >$ 4 Å. Figure 1b shows the vertical detachment energy (VDE) of an excess electron from the anionic state. Although several VDE curves can be drawn depending the combination of the anionic and neutral potentials, only one of those is plotted in Figure 1b since all the VDE curves were found to be very similar. The most important point is that the VDE value is almost constant independent of the C−I distance. This suggests that, in the case of so-called surface electron states, the VDE value is not strongly dependent on the distance between the I atom and the solvent cluster.

Figures 2 and 3 show the MRCI potential energy curves for the D_{3d}-like internal structure of the $I^-(CH_3CN)_2$ cluster as a function of different internal coordinates. Figure 2 displays the potential curves as a function of one of the C−I distance, which is defined in the figure. Note that the potential energy curves of the singlet and triplet CTTS states are purely repulsive both

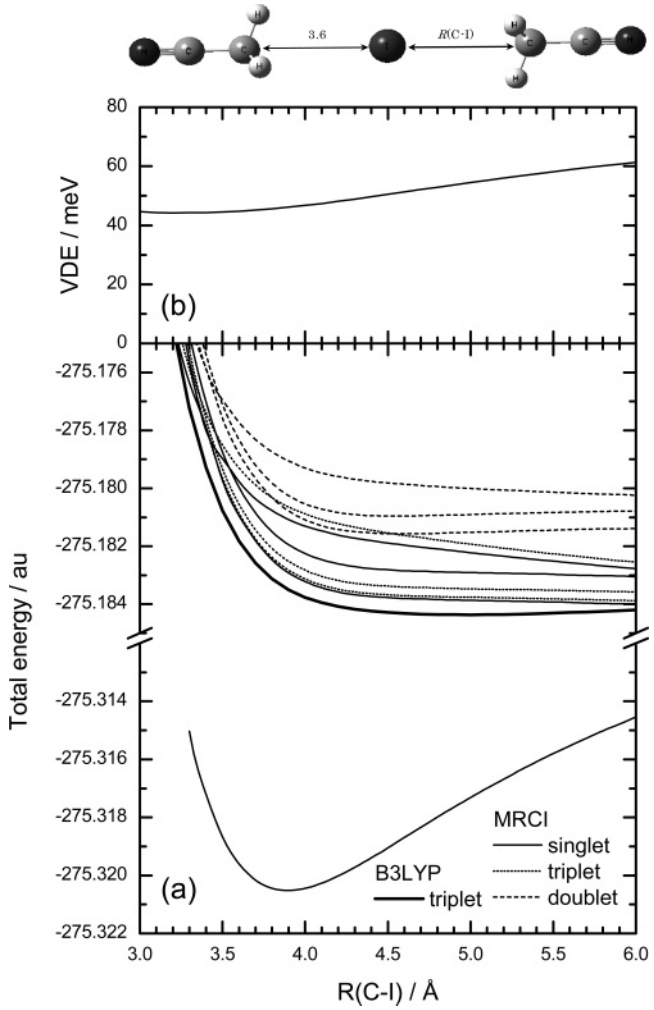

Figure 2. MRCI potential energy curves (a) as a function of the C−I distance for low-lying states of the $I^-(CH_3CN)_2$ and $I(CH_3CN)_2$ clusters with the D_{3d}-like internal configuration. B3LYP results for the lowest triplet state are shown as a bold line. The VDE value is also shown in (b). Plot convention is the same as Figure 1.

in the vertical excitation region and in the asymptotic region; however, it is seen that interaction energy is generally small, similar to the C_{3v}-like surface structure. It is interesting to notice that the VDE value slightly increases with the increase in the C−I distance. This indicates that the position of the I atom affects the spatial distribution of an excess electron in the cluster due to the "excluded volume" effect of the I atom.[31] Figure 3 shows the potential energy curves as a function of the iodide detachment coordinate *Z*, which is defined in the figure. Shallow local minima are seen at $Z \approx 2$ Å for both singlet and triplet CTTS states, but again, it is found that interaction energy is quite small. The VDE value is found to increase as *Z* increases. The results presented in Figures 2 and 3 imply that the effect of the iodide atom position on the VDE value cannot be ignored for the anion cluster, in which the I^- anion is internally solvated by molecules. It is expected that this finding may also be applicable to well-studied $I^-(H_2O)_n$ cluster cases.

IV. Photoexcitation Dynamics of the $I^-(CH_3CN)_n$ ($n = 2$ and 3) Clusters

Although we have presented MRCI potential energy curves of the CTTS excited states for the $I^-(CH_3CN)_2$ cluster in the previous section, it is still insufficient to understand the relaxation dynamics of the photoexcited $I^-(CH_3CN)_n$ cluster.

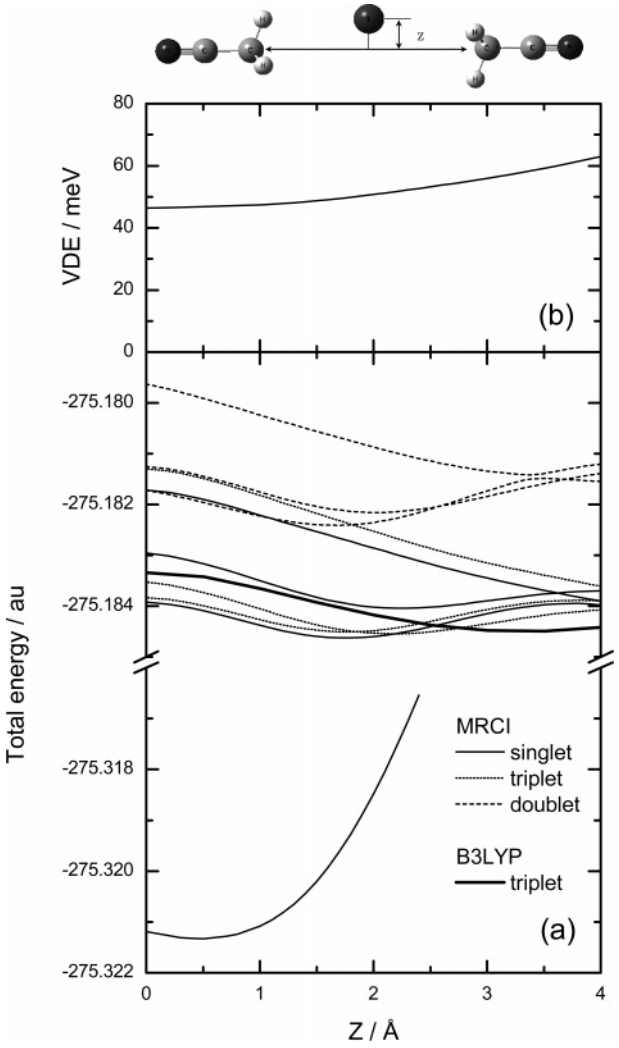

Figure 3. MRCI potential energy curves (a) as a function of the iodide detachment coordinate (Z) for low-lying states of the $I^-(CH_3CN)_2$ and $I(CH_3CN)_2$ clusters with the D_{3d}-like internal configuration. B3LYP results for the lowest triplet state are shown as a bold line. Plot convention is the same as Figure 1. The VDE value is also shown as a function of Z in (b).

To overcome this difficulty, we have carried out direct molecular dynamics calculations on the lowest triplet potential energy surface, which is found to be quite similar to the lowest singlet CTTS excited-state potential energy surface. To confirm the validity of using the lowest triplet potential energy surface at the B3LYP level, the potential energy curves for the $I^-(CH_3CN)_2$ cluster are compared to the MRCI results. The results are shown in Figures 1−3. Agreement between the B3LYP and MRCI results is seen to be reasonable, indicating that the B3LYP dynamics calculations are quite encouraging.

The molecular dynamics calculation was initiated with the cluster in its ground-state minimum-energy structure with no additional kinetic energy. Figure 4 shows the ground-state minimum-energy structures for the $I^-(CH_3CN)_n$ ($n = 2$ and 3) clusters, which were optimized at the B3LYP level of theory. Also shown are minimum-energy structures for the $(CH_3CN)_n^-$ anion clusters, for which the I^- anion was replaced by an excess electron distribution. The singly occupied molecular orbitals (SOMO) and the corresponding VDE values are also displayed in this figure.

Figure 5 shows the time evolution of the internuclear distances, total kinetic energy, and total electronic energy (potential energy) for the photoexcited D_{3d}-like internal

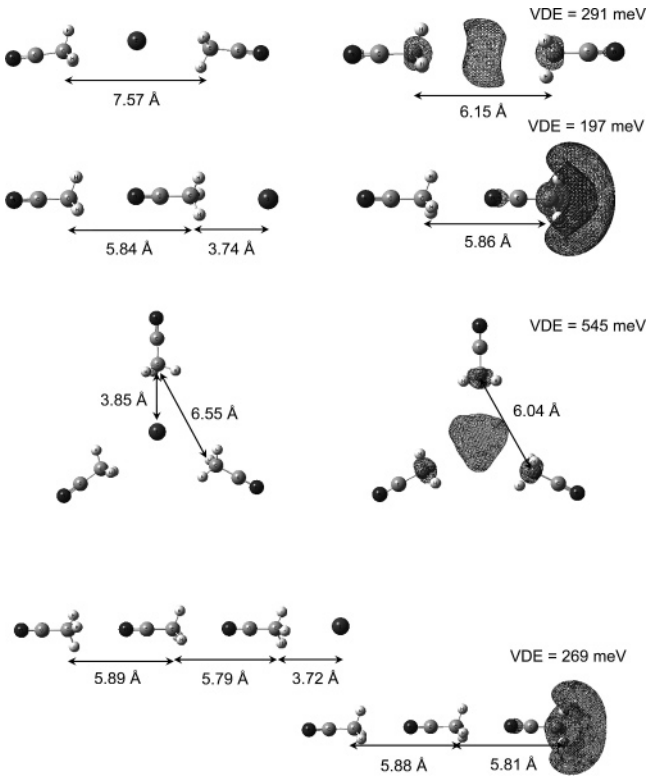

Figure 4. Minimum-energy structures for the $I^-(CH_3CN)_n$ and $(CH_3CN)_n^-$ ($n = 2$ and 3) clusters optimized at the B3LYP level of theory. Singly occupied molecular orbitals (SOMOs) for the $(CH_3CN)_n^-$ anion clusters are also shown to understand the excess electron distributions in the clusters.

$I^-(CH_3CN)_2$ cluster. Snapshots of some selected configurations and corresponding SOMOs along the trajectory are also presented. In this trajectory, it is seen that the photoexcited $I^-(CH_3CN)_2$ cluster simply dissociates into $I + CH_3CN^{(-)} + CH_3CN^{(-)}$. Thus, the process can be regarded as the three-body dissociation. At $t = 0$, the excess electron is distributed around the I atom. As acetonitrile molecules depart from the I atom, the excess electron gradually distributes around the methyl groups of acetonitrile molecules. Therefore, a so-called dipole-bound anion, for which an excess electron is bound by the large dipole field of CH_3CN, is formed in this trajectory. The obtained three-body dissociation dynamics can easily be predicted from the MRCI potential energy curves of the CTTS excited states showing a purely repulsive feature. Since no excess kinetic energy is introduced in this trajectory, the available energy is mainly distributed into the C−I stretch motions. However, notice that only a very small kinetic energy is partitioned into these coordinates. It should be mentioned that this trajectory was unfortunately terminated at $t \approx 610$ fs due to the SCF convergence problem. This is the result of a well-known symmetry-breaking problem, since the $I + CH_3CN^- + CH_3CN$ asymptotic state is doubly degenerate. This can be also understood from the fact that half of an excess charge is distributed in two CH_3CN molecules.

Figure 6 shows the same plot as Figure 5 but for the photoexcited C_{3v}-like asymmetric $I^-(CH_3CN)_2$ cluster. Unlike the trajectory presented in Figure 5, it is seen that the $(CH_3CN)_2^-$ anion cluster and I atom are finally formed in this trajectory. It was found that only 0.7 kcal/mol of energy is partitioned into the relative translational mode between $(CH_3CN)_2^-$ and the I atom. Thus, the translational motion of the I atom is quite slow; the distance between I and C in the terminal methyl group is about 5 Å even at $t = 500$ fs. It is also interesting to note that

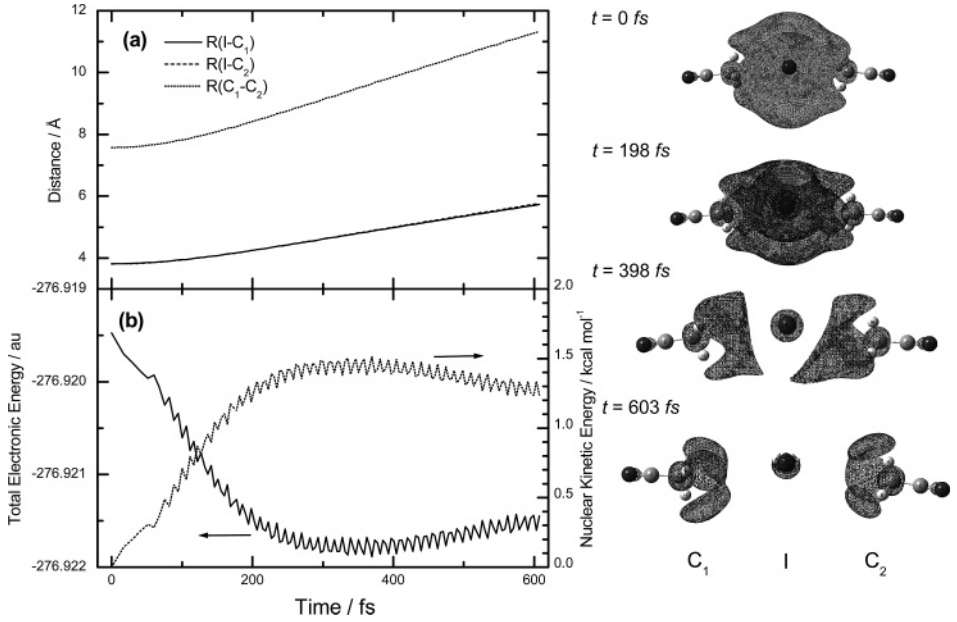

Figure 5. Time evolutions of the internuclear distances (a), total kinetic energy, and total electronic energy (b) for the photoexcited D_{3d}-like internal and symmetric $I^-(CH_3CN)_2$ cluster (left panel). Snapshots of selected configurations and corresponding SOMO plots are shown in the right panel.

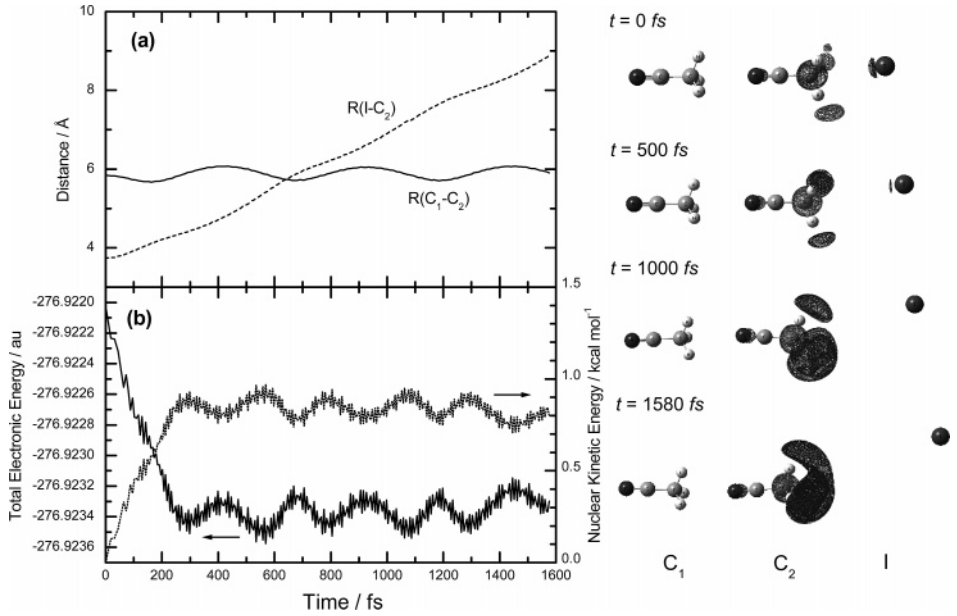

Figure 6. Time evolutions of the internuclear distances, total kinetic energy, and total electronic energy for the photoexcited C_{3v}-like surface $I^-(CH_3CN)_2$ cluster (left panel). Snapshots of selected configurations and corresponding SOMO plots are shown in the right panel.

the C−C distance oscillates in the range 5.7−6.1 Å with a period being about 600 fs. Notice that similar oscillations were seen in the time evolution of kinetic and potential energies. This slow motion corresponds to the intermolecular stretching motion between two acetonitrile molecules.

It should be important to give a more detailed comparison of the trajectory results presented in Figures 5 and 6 with the experimental work of refs 7 and 8 by Johnson and co-workers. In that work, it was reported that the $I^-(CH_3CN)_2$ cluster has two absorption bands with a differents intensities. Photoexcitation of the strong absorption band results in production of both CH_3CN^- and $(CH_3CN)_2^-$ anion fragments. On the other hand, excitation of the weak absorption band results in electron detachment. Johnson and co-workers concluded that the $I^-(CH_3CN)_2$ cluster has two isomers; the asymmetrically solvated $CH_3CN-CH_3CN-I^-$ configuration is responsible for the isomer with the strong absorption band, while the symmetrically solvated $NCCH_3-I^--H_3CCN$ structure can be identified as the isomer with a weak absorption band. These experimental findings are qualitatively consistent with the present BOMD calculations. However, notice that the electron detachment dynamics cannot be described by the present classical calculations. This should be an important issue to be addressed in the future.

We have also carried out molecular dynamics calculations for the $I^-(CH_3CN)_3$ cluster, and results are presented in Figures 7 and 8. Figure 7 shows the result for the photoexcited D_{3h}-like $I^-(CH_3CN)_3$ cluster, where the I^- anion is internally trapped by three acetonitrile molecules. The dynamics is essentially the same as the result presented in Figure 5. It is seen that three acetonitrile molecules gradually detach from the central I atom, although the kinetic energy is not so large. Figure 8 shows the

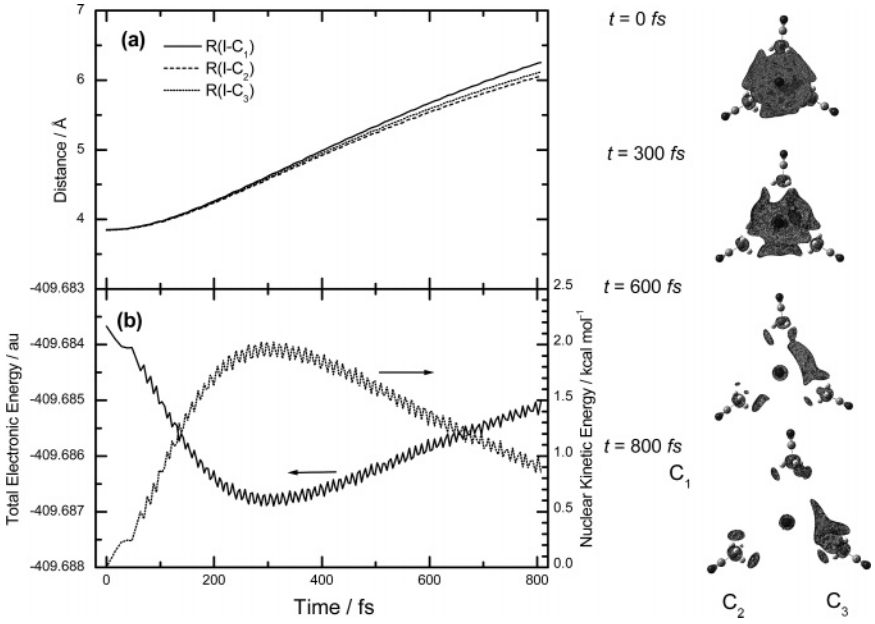

Figure 7. Time evolutions of the internuclear distances, total kinetic energy, and total electronic energy for the photoexcited D_{3h}-like internal $I^-(CH_3CN)_3$ cluster (left panel). Snapshots of selected configurations and corresponding SOMO plots are shown in the right panel.

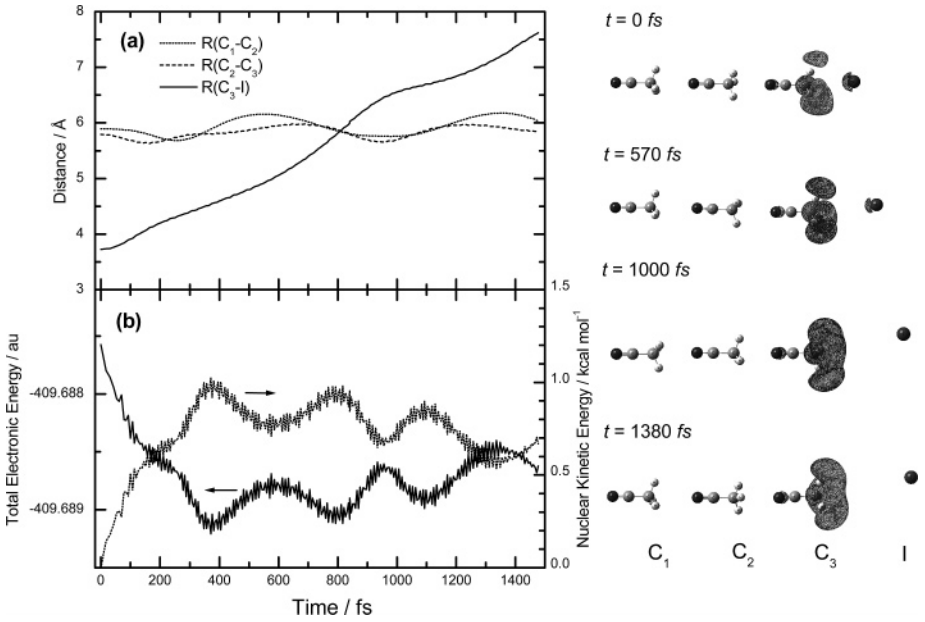

Figure 8. Time evolutions of the internuclear distances, total kinetic energy, and total electronic energy for the photoexcited C_{3v}-like surface $I^-(CH_3CN)_3$ cluster (left panel). Snapshots of selected configurations and corresponding SOMO plots are shown in the right panel.

molecular dynamics result for the photoexcited C_{3v}-like $I^-(CH_3CN)_3$ cluster, and the dynamics is very similar to the dynamics shown in Figure 6. Slow oscillations corresponding to intermolecular motions can be seen in the time evolution of the C_1-C_2 and C_2-C_3 distances as well as the kinetic and potential energies.

From the results presented in Figures 5−8, it can be concluded that photoexcitation of the $I^-(CH_3CN)_n$ cluster to the CTTS excited state effectively yields the $(CH_3CN)_n^-$ cluster anion when the I^- anion is externally solvated. This result can be easily expected since the initial configuration of acetonitrile molecules is quite similar to that in the $(CH_3CN)_n^-$ anion clusters. On the other hand, in the case of the $I^-(CH_3CN)_n$ cluster, where the I^- anion is internally solvated, photoexcitation does not produce $(CH_3CN)_n^-$ anion clusters. However, it should be noticed that the above molecular dynamics calculations were carried out with no excess energy and that the initial configuration was fixed at the minimum structure of the ground-state $I^-(CH_3CN)_n$ cluster. In usual experimental conditions, the $I^-(CH_3CN)_n$ cluster should have a finite internal temperature (internal energy). This suggests that there is the possibility that the initial configuration of $I^-(CH_3CN)_n$ may be somewhat distorted from the equilibrium configuration.

To understand the effect of the initial configuration on photoexcitation dynamics, we have performed additional molecular dynamics calculations. First, we have done BOMD calculations for the D_{3d}-like symmetric $I^-(CH_3CN)_2$ cluster, where the I^- anion is internally solvated between two acetonitrile molecules, on the ground-state singlet potential energy surface at the B3LYP level. At the start of the trajectory calculation, atomic velocities were adjusted to give a temperature of about 50 K, and the molecular dynamics calculation was performed during about 2 ps. Next, some of geometric configurations and corresponding atomic velocities were chosen from this calcula-

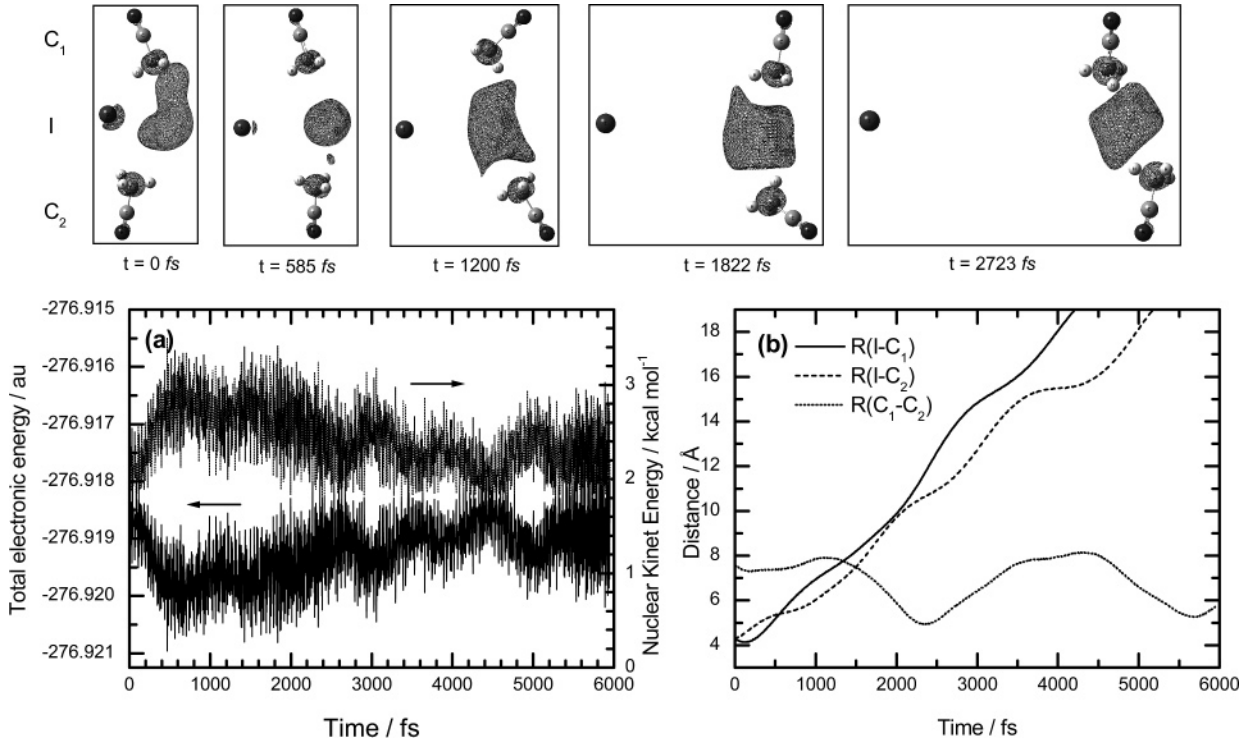

Figure 9. Same as Figure 5, but the initial configuration and kinetic energy were chosen from the molecular dynamics simulation on the ground-state singlet potential energy surface. It is seen that the $(CH_3CN)_2^-$ anion cluster, where an excess electron is internally trapped by the two methyl groups, is finally formed in this trajectory.

tion, and then, BOMD calculation with the selected initial condition was done on the assumption of vertical excitation to the triplet CTTS state. One of the results of those calculations is displayed in Figure 9. Notice that the initial I atom position is somewhat displaced from the center of the two acetonitrile molecules and that the initial kinetic energy is about 2 kcal/mol. Interestingly, the $(CH_3CN)_2^-$ dimer anion is clearly formed in this trajectory at $t \approx 2$ ps after photoexcitation. Note that the calculation was done for a very long time in order to confirm the dimer anion production. We can see the very large-amplitude motion for the C_1-C_2 intermolecular stretch in the range of about 5−8 Å. Also, this motion is found to have very a long period of about 3.5 ps. This means that the excess electron distribution is also oscillating with the same period. The result of this calculation indicates that the CTTS relaxation dynamics is strongly dependent on the initial geometric configuration of the $I^-(CH_3CN)_2$ cluster. Since we have done only a few dynamics calculations due to computational costs and did not systematically (or randomly) select the initial configurations, there is no statistical information on the product branching ratio. At least for the D_{3d}-like $I^-(CH_3CN)_2$ cluster, it is presumed that the $(CH_3CN)_2^-$ dimer anion production channel is minor. We have also carried out similar dynamics calculations for the D_{3h}-like $I^-(CH_3CN)_3^-$ cluster; however, we did not find the $(CH_3CN)_3^-$ cluster anion production. Nevertheless, it may be interesting to obtain a large number of trajectories in order to understand the overall relaxation mechanism. In addition, it should be interesting to extend the present dynamics calculations to larger $I^-(CH_3CN)_n$ ($n > 3$) clusters, since there is the possibility that photoexcitation of large $I^-(CH_3CN)_n$ clusters may produce the $(CH_3CN)_m^-$ anion cluster with a different number of acetonitrile molecules via $I^-(CH_3CN)_n + h\nu \rightarrow (CH_3CN)_m^- + (n-m)CH_3CN$ process. Such dynamics calculations are now in progress in our laboratory. Also, it should be interesting to apply the present computational technique to the photoexcitation dynamics of the well-studied $I^-(H_2O)_n$ clusters, for which extensive femtosecond experimental studies[11−17] are available, as mentioned in the Introduction.

V. Conclusions

We have studied relaxation dynamics of the CTTS excited state of the $I^-(CH_3CN)_n$ ($n = 2$ and 3) clusters using the direct molecular dynamics technique. Since the MRCI calculations of the CTTS excited-state potential energy surfaces show that the features of the singlet CTTS excited states are very similar to those of the triplet CTTS states, the dynamics calculations were carried out on the lowest triplet potential energy surface, which has been obtained at the B3LYP level of theory.

The $I^-(CH_3CN)_n$ clusters have two important geometric configurations: one with the solvent molecules surrounding the I^- anion and another with both solvent molecules on the same side, asymmetrically solvating I^-. Notice that the former has a small electric dipole moment, while the latter has a large dipole moment. The present molecular dynamics simulations show that photoexcitation of the former-type clusters to the CTTS state does not yield the $(CH_3CN)_n^-$ anion clusters. On the other hand, photoexcitation of the latter-type clusters effectively produces the $(CH_3CN)_n^-$ anion cluster, for which an excess electron is bound by a large dipole field of the $(CH_3CN)_n$ cluster in a nearly linear head-to-tail configuration. However, the detachment process of the neutral I atom from the $(CH_3CN)_n^-$ anion cluster is found to be generally slow due to a small amount of kinetic energy partitioned into the dissociation mode. This result can be partly expected from the flatness of the CTTS potential energy surfaces obtained at the MRCI level. We have also carried out molecular dynamics simulations of the D_{3d}-like symmetric $I^-(CH_3CN)_2$ cluster, for which the initial configuration was somewhat deformed from the equilibrium geometry. Interestingly, we have observed the $(CH_3CN)_2^-$ anion cluster production, where an excess electron is internally solvated by two methyl groups of acetonitrile. Although this process is

expected to be minor, our calculation suggests that the relaxation dynamics is dependent on the initial geometric configuration of the $I^-(CH_3CN)_2$ cluster in the ground electronic state.

Although additional theoretical calculations would be necessary to understand the statistical information such as product branching, we hope that the present theoretical dynamics calculations stimulate further experimental studies. Also, it should be important to apply the present computational technique to the well-studied $I^-(H_2O)_n$ system. Work along this line is now progress in our laboratory.

Acknowledgment. This work was supported partly by the Grant-in-Aid for Scientific Research of the Ministry of Education, Culture, Sports, Science, and Technology of Japan (grant no. 17550007).

References and Notes

(1) Coe, J. V. *Int. Rev. Phys. Chem*. **2001**, *20*, 33.
(2) Sheu, W.-S.; Rossky, P. J. *Chem. Phys. Lett*. **1993**, *213*, 233.
(3) Sheu, W.-S.; Rossky, P. J. *J. Am. Chem. Soc*. **1993**, *115*, 7729.
(4) Sheu, W.-S.; Rossky, P. J. *J. Phys. Chem*. **1996**, *100*, 1295.
(5) Staib, A.; Borgis, D. *J. Chem. Phys*. **1995**, *103*, 2642.
(6) Simons, J.; Jordan, K. D. *Chem. Rev*. **1987**, *87*, 535.
(7) Dessent, C. E. H.; Bailey, C. G.; Johnson, M. A. *J. Chem. Phys*. **1995**, *103*, 2006.
(8) Dessent, C. E. H.; Kim, J.; Johnson, M. A. *J. Phys. Chem*. **1996**, *100*, 12.
(9) Bailey, C. G.; Dessent, C. E. H.; Johnson, M. A.; Bowen, K. H., Jr. *J. Chem. Phys*. **1996**, *104*, 6976.
(10) Serxner, D.; Dessent, C. E. H.; Johnson, M. A. *J. Chem. Phys*. **1996**, *105*, 7231
(11) Lehr, L.; Zanni, M. T.; Frischkorn, C.; Weinkauf, R.; Neumark, D. M. *Science* **1999**, *284*, 635.
(12) Frischkorn, C.; Zanni, M. T.; Davis, A. V.; Neumark, D. M. *Faraday Discuss*. **2000**, *115*, 49.
(13) Zanni, M. T.; Frischkorn, C.; Davis, A. V.; Neumark, D. M. *J. Phys. Chem. A* **2000**, *104*, 2527.
(14) Davis, A. V.; Zanni, M. T.; Weinkauf, R.; Neumark, D. M. *Chem. Phys. Lett*. **2002**, *353*, 455.
(15) Kammrath, A.; Verlet, J. R. R.; Bragg, A. E.; Griffin, G. B.; Neumark, D. M. *J. Phys. Chem. A* **2005**, *109*, 11475.
(16) Verlet, J. R. R.; Kammrath, A.; Griffin, G. B.; Neumark, D. M. *J. Chem. Phys*. **2005**, *123*, 1.
(17) Szpunar, D. E.; Kautzman, K. E.; Faulhaber, A. E.; Neumark, D. M. *J. Chem. Phys*. **2006**, *124*, 1.
(18) Majumdar, D.; Kim, J.; Kim, K. S. *J. Chem. Phys*. **2000**, *112*, 101.
(19) Kim, J.; Lee, H. M.; Suh, S. B.; Majumdar, D.; Kim, K. S. *J. Chem. Phys*. **2000**. *113*, 5259.
(20) Lee, H. M.; Kim, K. S. *J. Chem. Phys*. **2001**, *114*, 4461.
(21) Lee, H. M.; Suh, S. B.; Kim, K. S. *J. Chem. Phys*. **2002**, *116*, 5509.
(22) Lee, H. M.; Suh, S. B.; Kim, K. S. *J. Chem. Phys*. **2002**, *118*, 9981.
(23) Lee, H. M.; Suh, S. B.; Kim, K. S. *J. Chem. Phys*. **2003**, *119*, 7685.
(24) Kołaski, M.; Lee, H. M.; Pak, C.; Dupuis, M.; Kim, K. S. *J. Phys. Chem. A* **2005**, *109*, 9419.
(25) Bergner, A.; Dolg, M.; Kuechle, W.; Stoll, H.; Preuss, H. *Mol. Phys*. **1993**, *80*, 1431.
(26) Glukhovtsev, M. N.; Pross, A.; McGrath, M. P.; Radom, L. *J. Chem. Phys*. **1995**, *103*, 1878.
(27) Kendall, R. A.; Dunning, T. H., Jr.; Harrison, R. J. *J. Chem. Phys*. **1996**, *96*, 6796.
(28) Takayanagi, T. *J. Chem. Phys*. **2005**, *122*, 244307.
(29) Amos, R. D.; Bernhardsson, A.; Berning, A.; Celani, P.; Cooper, D. L.; Deegan, M. J. O.; Dobbyn, A. J.; Eckert, F.; Hampel, C.; Hetzer, G.; Knowles, P. J.; Korona, T.; Lindh, R.; Lloyd, A. W.; McNicholas, S. J.; Manby, F. R.; Meyer, W.; Mura, M. E.; Nicklass, A.; Palmieri, P.; Pitzer, R.; Rauhut, G.; Schütz, M.; Schumann, U.; Stoll, H.; Stone, A. J.; Tarroni, R.; Thorsteinsson, T.; Werner, H.-J. *MOLPRO*, a package of ab initio programs designed by Werner, H.-J. and Knowles, P. J., version 2002.1.
(30) Timerghazin, Q.; Peslherbe, G. H. *J. Am. Chem. Soc*. **2003**, *125*, 9904.
(31) Bradforth, S. E.; Jungwirth, P. *J. Phys. Chem. A* **2002**, *106*, 1286.
(32) Villa, F. D.; Jordan, K. D. *J. Phys. Chem*. **2002**, *106*, 1391.
(33) Becke, A. D. *J. Chem. Phys*. **1993**, *98*, 5648.
(34) Frisch, M. J.; Trucks, G. W.; Schlegel, H. B.; Scuseria, G. E.; Robb, M. A.; Cheeseman, J. R.; Montgomery, Jr., J. A.; Vreven, T.; Kudin, K. N.; Burant, J. C.; Millam, J. M.; Iyengar, S. S.; Tomasi, J.; Barone, V.; Mennucci, B.; Cossi, M.; Scalmani, G.; Rega, N.; Petersson, G. A.; Nakatsuji, H.; Hada, M.; Ehara, M.; Toyota, K.; Fukuda, R.; Hasegawa, J.; Ishida, M.; Nakajima, T.; Honda, Y.; Kitao, O.; Nakai, H.; Klene, M.; Li, X.; Knox, J. E.; Hratchian, H. P.; Cross, J. B.; Adamo, C.; Jaramillo, J.; Gomperts, R.; Stratmann, R. E.; Yazyev, O.; J. Austin, A.; Cammi, R.; Pomelli, C.; Ochterski, J. W.; Ayala, P. Y.; Morokuma, K.; Voth, G. A.; Salvador, P.; Dannenberg, J. J.; Zakrzewski, V. G.; Dapprich, S.; Daniels, A. D.; Strain, M. C.; Farkas, O.; Malick, D. K.; Rabuck, A. D.; Raghavachari, K.; Foresman, J. B.; Ortiz, J. V.; Cui, Q.; Baboul, A. G.; Clifford, S.; Cioslowski, J.; Stefanov, B. B.; Liu, G.; Liashenko, A.; Piskorz, P.; Komaromi, I.; Martin, R. L.; Fox, D. J.; Keith, T.; Al-Laham, M. A.; Peng, C. Y.; Nanayakkara, A.; Challacombe, M.; Gill, P. M. W.; Johnson, B.; Chen, W.; Wong, M. W.; Gonzalez, C.; Pople, J. A. *Gaussian 03*, revision C.02; Gaussian, Inc.: Wallingford, CT, 2004.
(35) Herbert, J. M.; Head-Gordon, M. *J. Phys. Chem. A* **2005**, *109*, 5217.
(36) Herbert, J. M.; Head-Gordon, M. *Phys. Chem. Chem. Phys*. **2006**, *8*, 68.
(37) Timerghazin, Q. K.; Nguyen, T.-N.; Peslherbe, G. H. *J. Chem. Phys.* **2002**, *116*, 6867.
(38) Timerghazin, Q. K.; Peslherbe, G. H. *Chem. Phys. Lett*. **2002**, *354*, 31.
(39) Nguyen, T.-N.; Peslherbe, G. H. *J. Phys. Chem. A* **2003**, *107*, 1540.